1-1-1996

Early Spectra of the Supernova 1987F

Gary Wegner
Dartmouth College

Steven R. Swanson
Dartmouth College

Mon. Not. R. Astron. Soc. **278,** 22–38 (1996)

Early spectra of the supernova 1987F

Gary Wegner[1,2,3] and Steven R. Swanson[3]

[1]*Astronomisches Institut, Ruhr-Universität Bochum, D-44780 Bochum, BRD*
[2]*Department of Astrophysics, Keble Road, Oxford OX1 3RQ*
[3]*Department of Physics and Astronomy, Dartmouth College, Wilder Laboratory, Hanover, New Hampshire 03755, USA*

Accepted 1995 July 25. Received 1995 July 24; in original form 1994 July 15

ABSTRACT

Spectroscopy is presented of the peculiar Type II supernova 1987F, sometimes called the 'Type I Seyfert imposter'. This supernova differed from others of Type II in the slow evolution in its light curve and the strengths and profiles of the spectral lines. The time covered is 1987 April 2 to June 8, when the spectrum of the supernova evolved from a simple nearly featureless blue continuum with superimposed narrow emission lines of H I, He I, [N II], [O III], and [S II] to a complicated combination of broad and narrow emission components in H I and He I plus the wide features identified by earlier authors as being caused by Fe II. Using a simple model of an expanding spherical shell with absorption for the broad Hα and Hβ lines, an expansion speed of ~ 8000 km s^{-1} is estimated for the outer surface of the shell. This expansion velocity, combined with the mean density of the shell derived three ways, predicts a mass of $\sim 0.2\,M_{\odot}$ for the ejected hydrogen above the photosphere. The He abundance appears to be enhanced in this object. The unusual light curve indicates a total luminous energy of $\sim 10^{51}$ erg. After 50 d, its shape can be fitted either by a model using a shockwave expanding into circumstellar material, by $^{56}Ni \rightarrow {}^{56}Co \rightarrow {}^{56}Fe$ decay with a reddening and radiative transfer dependent mass of 0.8 to 2.6 $M_{\odot}$ for the ^{56}Ni, or both. Such a high amount of ^{56}Ni suggests that other mechanisms are involved. Possible processes leading to SN 1987F are explored and the suggested link between this object and AGNs is also briefly discussed.

Key words: line: profiles – techniques: spectroscopic – supernovae: individual: 1987F – galaxies: individual: NGC 4615.

1 INTRODUCTION

Metlova (Cherepaschuk & Metlova 1987) discovered the supernova 1987F in NGC 4615 [$\alpha_{2000} = 12^h41^m37^s.6$, $\delta_{2000} = +26°04'29''$, $V_{21} = 4716 \pm 9$ km s^{-1}, type Scd (de Vaucouleurs et al. 1991)] on 1987 March 22 at about 20 arcsec east of the nucleus and Wild & Schildknecht (1987) independently located it on 23 April, putting it 24 arcsec east and 6 arcsec south. SN 1987F was unusual both from the appearance and development of its spectrum (Cherepaschuk et al. 1987; Wegner & Swanson 1988) and the slow decline in light.

The appearance of the spectrum after 1987 May 3 and the shape of the light curve are described further in Filippenko & Schachter (1988), Filippenko (1989), Tsvetkov (1989), Cappellaro et al. (1990), and Patat et al. (1993). By this time, SN 1987F showed a strong continuum and Balmer lines of impressive strength. Using a later spectrum of SN 1987F, Filippenko (1989) discussed the similarities between it and the spectra of a typical Seyfert I and a radio-quiet QSO.

The slow decline of light in SN 1987F and its unusual spectrum led Wegner & Swanson (1988) to point out similarities with Zwicky's (1965) Type III supernovae. The photometry in Filippenko (1989) and Cappellaro et al. (1990) show that even 400 d after discovery, the V and B magnitudes had only faded by about 2.5 mag. Both of these studies showed that SNe II-P and SNe II-L (Barbon, Ciatti & Rosino 1979; Doggett & Branch 1985) fade faster than this and surmised that such a slow decay rate could indicate a massive progenitor for SN 1987F, as did Tsvetkov (1989).

Chugai (1991) reached similar conclusions by modelling the Hα luminosity of SN 1987F and interpreted the observed properties as being caused by an unusually strong ejecta–wind interaction, possibly owing to a heavy mass-loss prior to the supernova.

Additional Type II supernovae with some of the unusual

properties peculiar to SN 1987F have now been recognized. These include SN 1988Z (Turatto et al. 1993) and a handful of others listed by Schlegel (1990) who proposed that these supernovae comprise a new 'Type IIn' subclass. This type of supernova also features in the AGN model proposed by Terlevich et al. (1992).

Spectroscopy of SN 1987F was obtained at earlier phases than reported previously from 1987 April 2 to 1987 June 8 at the Michigan–Dartmouth–MIT (MDM) Observatory. These data are described in Sections 2 and 3 and show further remarkable properties of this unusual supernova. Some estimates of the physical properties of SN 1987F and their possible use as clues to the nature of its progenitor are given in Section 4.

2 OBSERVATIONS

Table 1 gives a journal of the spectroscopic observations of SN 1987F obtained with the telescopes at the MDM Observatory on Kitt Peak. All spectra with the 1.3-m McGraw-Hill telescope were made using the Mark II spectrograph. This employed a 2048-channel photon counting Reticon detector system and a six-stage fibre-optically coupled electrostatic image-tube (cf. Schechtman & Hiltner 1976). A 2.8-arcsec diameter entrance hole and a 300 lines mm^{-1} grating were used, giving about 8 Å resolution and covering the $\lambda\lambda$4000–7200 Å wavelength region.

Table 1. Log of observations for SN 1987F.

1987 UT date	UT Mid.	Exp(s)	Tel.	Inst. setup	Obs.
02 Apr	6:51	3948	1.3m	C	SRS
02 Apr	7:00	1800	2.4m	A	GW
03 Apr	7:12	4854	1.3m	C	SRS
03 Apr	4:00	2400	2.4m	A	GW
05 Apr	5:48	2400	1.3m	C	SRS
05 Apr	3:00	1200	2.4m	A	GW
07 Apr	4:41	2400	1.3m	C	SRS
07 Apr	3:00	1200	2.4m	A	GW
08 Apr	4:00	1200	2.4m	A	GW
08 Apr	4:35	2400	2.4m	C	SRS
09 Apr	3:00	1500	2.4m	A	GW
10 Apr	3:53	2400	1.3m	C	SRS
10 Apr	7:48	2376	1.3m	C	SRS
11 Apr	3:46	2400	1.3m	C	SRS
14 Apr	4:09	4140	1.3m	C	SRS
15 Apr	3:58	2688	1.3m	C	SRS
16 Apr	4:02	2688	1.3m	C	SRS
17 Apr	3:52	3000	1.3m	C	SRS
18 Apr	3:54	3000	1.3m	C	SRS
20 Apr	4:46	3000	1.3m	C	SRS
27 May	3:00	1800	2.4m	B	GW
28 May	4:00	1800	2.4m	B	GW
29 May	3:00	1800	2.4m	B	GW
30 May	3:00	1800	2.4m	A	GW
31 May	3:00	1800	2.4m	A	GW
01 Jun	3:00	1800	2.4m	A	GW
02 Jun	3:00	1800	2.4m	A	GW
03 Jun	3:00	1800	2.4m	B	GW
08 Jun	3:00	1800	2.4m	B	GW

Notes to Table 1.
The instrumental setups are as follows: (A) 2.4-m telescope and Mark III spectrograph with 600 line mm^{-1} grism; (B) 2.4-m telescope and Mark III spectrograph with 300 line mm^{-1} grism; (C) 1.3-m telescope using Mark II spectrograph.

Observations obtained with the 2.4-m Hiltner telescope were made using the Mark III spectrograph which employed glass optics, a grism, and an RCA SID501EX CCD as the detector. A 1.9-arcsec slit running north–south was used with either a 300 line mm^{-1} or a 600 line mm^{-1} grism. The former grism covered the wavelength range of approximately $\lambda\lambda$4000–7200 with 12 Å resolution while the latter yielded 6 Å resolution over $\lambda\lambda$4800–6250. Further details on both instruments and reductions can be found in Wegner & Swanson (1990).

All spectra were reduced at Dartmouth using standard procedures. For the CCD data, the IRAF[1] package (Tody 1986) with a full two-dimensional sky subtraction was used, while for the 1.3-m Reticon observations, the REDUCE/INTERACT package (Maker, Kurtz & LaSala 1982) was employed. In all cases, bias subtraction, flattening using tungsten lamp spectra, transforming to the true wavelength-scale, correcting for the atmospheric extinction using mean values for the wavelength dependence at Kitt Peak, and converting to true flux from observations of flux standard stars were carried out. All fluxes reported in this paper are F_λ which is the flux per wavelength interval.

Plots of the reduced spectra are arranged in the time sequences shown in Figs 1–7. Figs 1–3 display the 1.3-m data and all except Fig. 1 are on a linear scale. Figs 4–7 show the same for the 2.4-m spectra. Figs 4 and 5 give the wavelength region $\lambda\lambda$4800–6200 as observed with the higher-resolution 600 line mm^{-1} grism but with portions of 300 line mm^{-1} spectra plotted to the same scale. Fig. 6 shows the entire wavelength range of the 300 line mm^{-1} spectra from the 2.4-m telescope.

The resulting signal-to-noise ratio in the 1.3-m spectra of SN 1987F was about 15–20 per pixel near λ5500 in the continuum, while the corresponding signal-to-noise ratio achieved with the CCD and 2.4-m telescope was about 50 per pixel. This means that in looking at these spectra, wide features covering many pixels such as the broad Hβ and Fe II are real, but spikes of only 1–2 pixel in width and near the noise level of the continuum which vary from night to night cannot be counted as real.

Fig. 7 shows summations of the two sets of 2.4-m spectra for the wavelength interval $\lambda\lambda$4750–6250. These have been normalized to a continuum estimated by fitting a smooth curve to the overall shape of the spectrum and have higher signal-to-noise ratios, but sacrifice the time resolution. Fig. 8 is an enlargement of the Hα spectral region for the spectra in Fig. 6 and identifications discussed below are indicated.

Knowing what is contributed separately by the supernova and the background galaxy is one difficulty with many supernova observations. While it is not expected that the blue continuum and broad emission lines arise from this background, this is not necessarily the case for the narrow lines. If the background near the supernova has a grainy unresolved structure, slight nightly differences in placing the slit and variations in the seeing can produce apparent changes in the

[1]IRAF is distributed by the National Optical Astronomy Observatories which is operated by the Association of Universities for Research in Astronomy, Inc. under contract with the National Science Foundation.

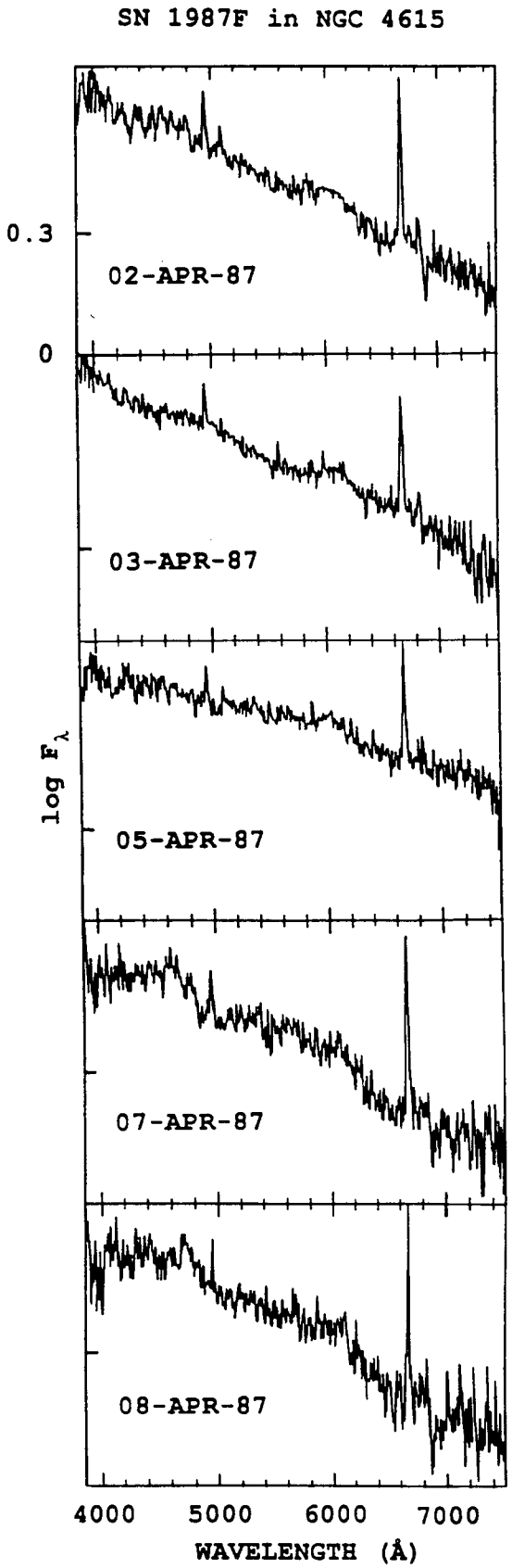

Figure 1. Spectral scans of the SN 1987F made with the 1.3-m McGraw-Hill telescope. The abscissae are plotted logarithmically in F_λ and from the bottom of each panel to the tick mark represents 0.3 in $\Delta \log F_\lambda$. All dates are GMT.

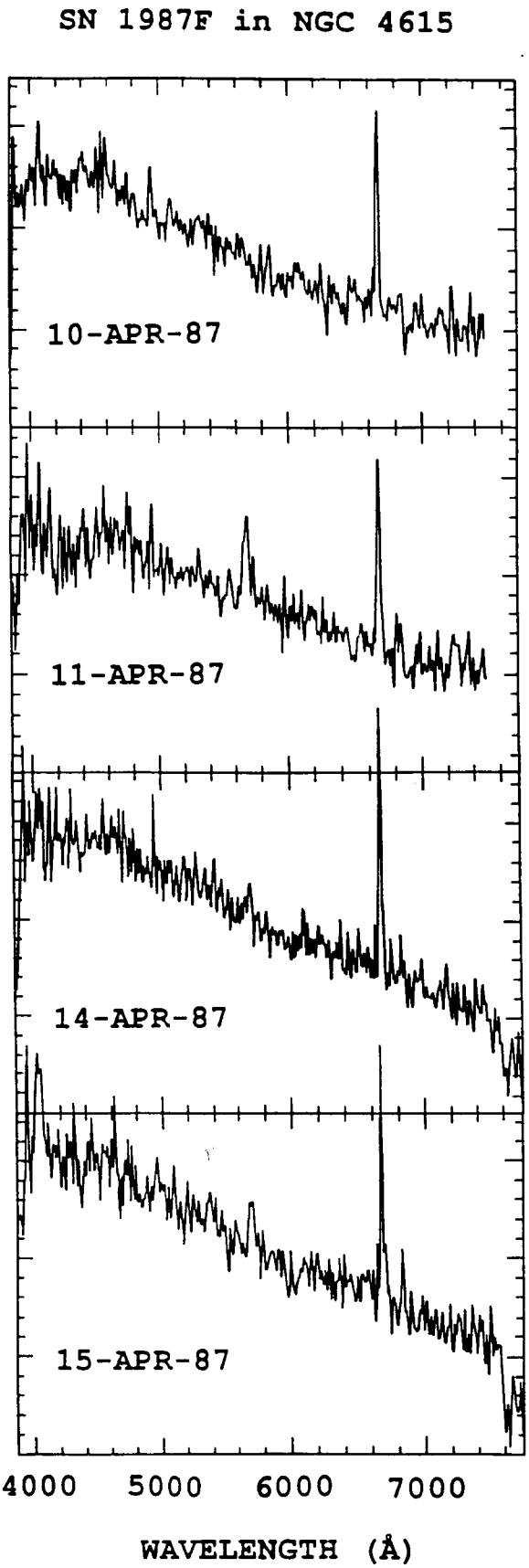

Figure 2. Further spectra of SN 1987F from the McGraw-Hill 1.3-m Telescope. Plots are linear in relative intensity F_λ and zero intensity is given at the bottom of each panel.

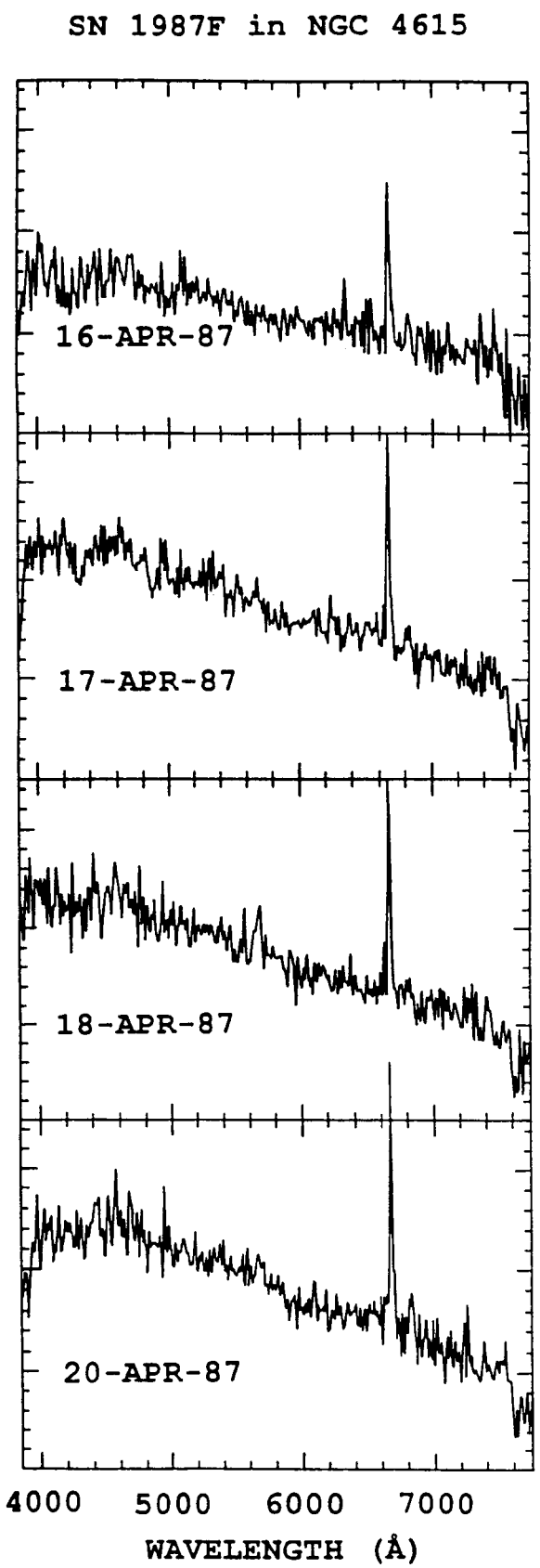

Figure 3. Further spectra of SN 1987F as in Fig. 2.

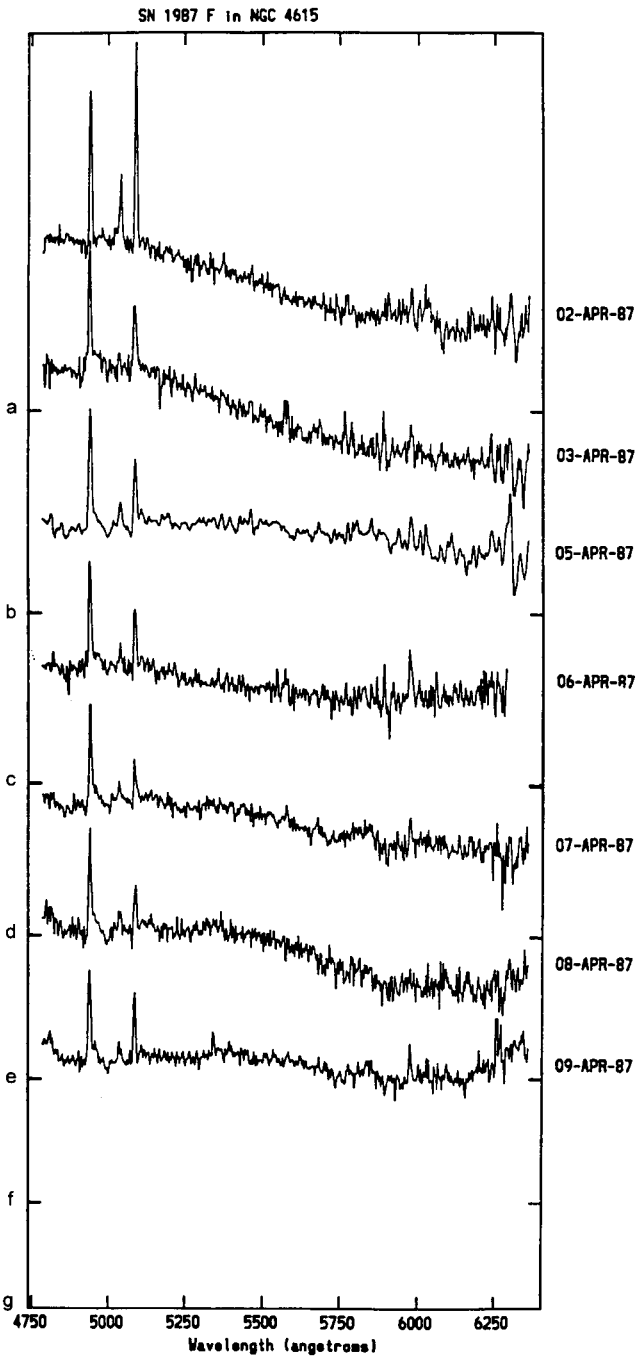

Figure 4. Spectra of SN 1987F obtained during April 1987 with the Hiltner 2.4-m telescope using the Mark III spectrograph and a 600 line mm^{-1} grism. The plots are linear in relative intensity F_λ. Zero intensity is denoted by the ticks a–g corresponding to each spectral registration running from the top to the bottom of the diagram.

narrow lines. Fig. 9 gives the spectrum of NGC 4615 in the spiral arm opposite the nucleus from SN 1987F and at the same radial distance. Narrow Hα emission is definitely present, but weaker than in the supernova spectrum and illustrates this difficulty. If this is representative of the background of this galaxy in the vicinity of the SN 1987F, there is a contribution of about 5–10 per cent, through the

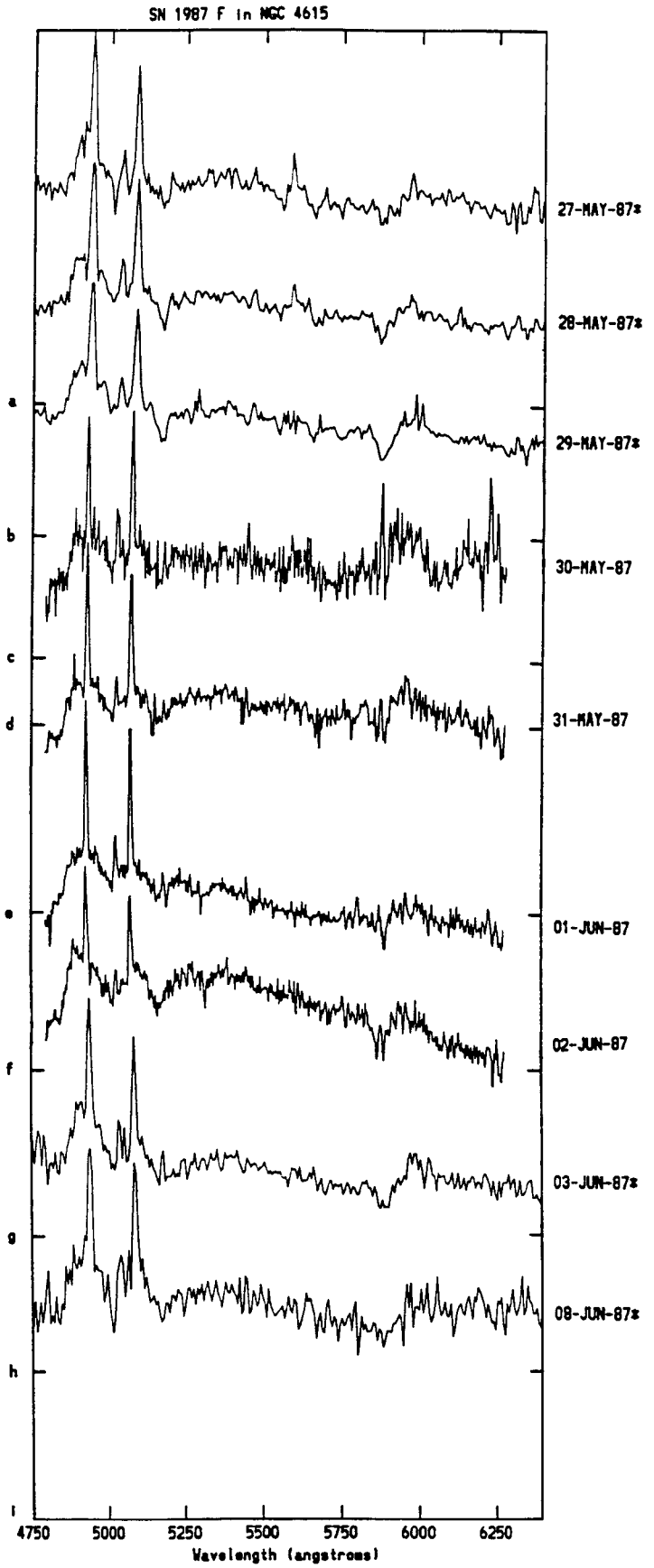

Figure 5. As in Fig. 4, but for the 1987 May–June MDM run. Scans with dates followed by an asterisk were obtained with a 300 line mm^{-1} grism.

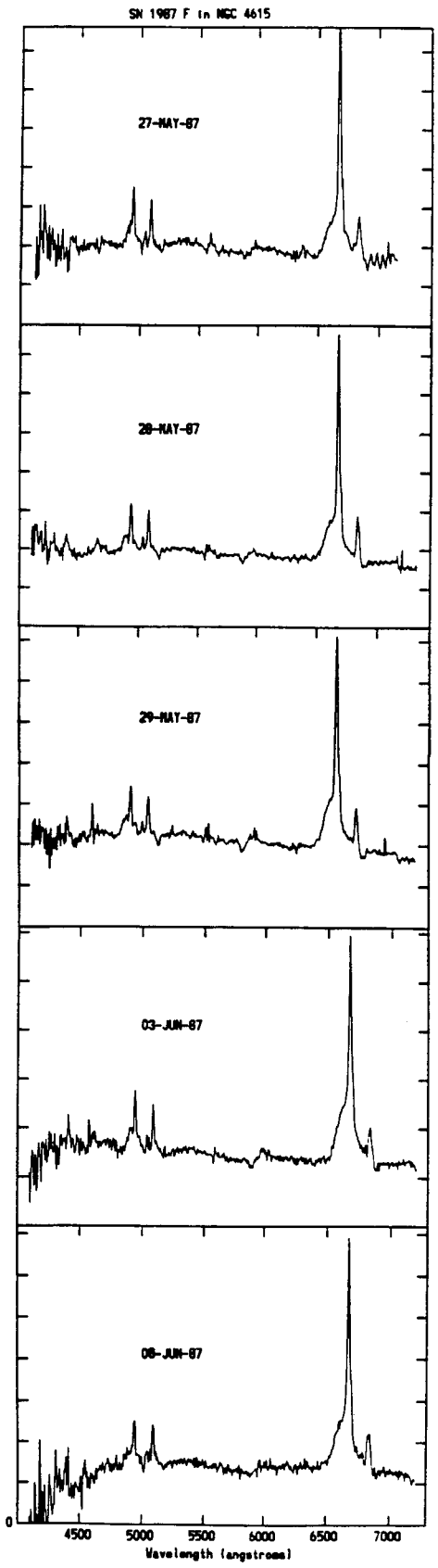

Figure 6. Plots of the entire lower-resolution 300 line mm^{-1} spectra obtained during 1987 May–June with the MDM 2.4-m telescope and showing the strong Hα line in emission. Zero intensity is at the bottom of each panel.

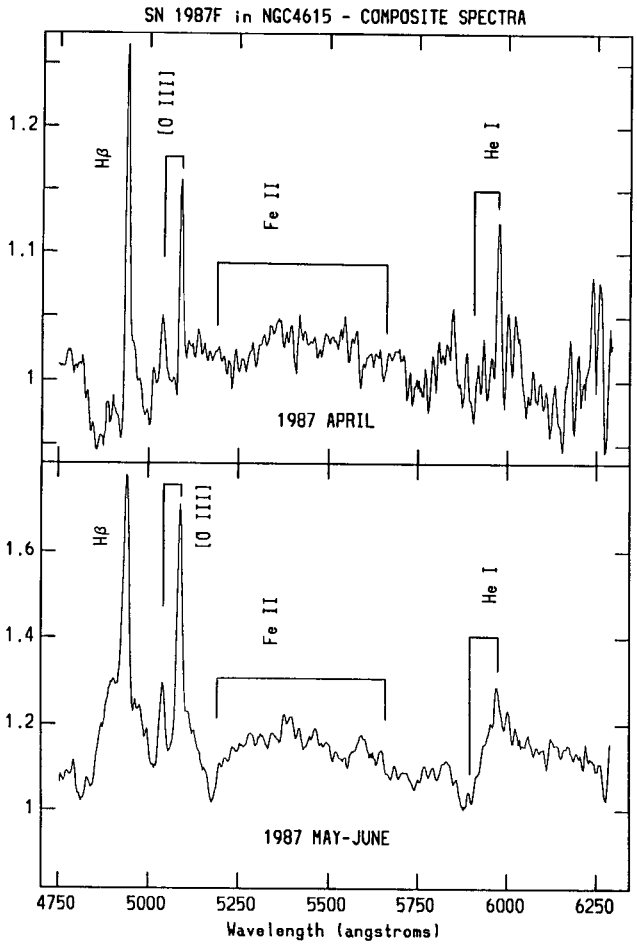

Figure 7. The sum of the 2.4-m spectra relative to the estimated continuum at 1.0. The top panel shows the sum of all individual spectra in Fig. 4 taken during 1987 April and the bottom panel shows those in Figs 5 and 6 taken 1987 May–June. Identifications of features discussed in the text are indicated. In the bottom panel both high- and low-resolution data have been averaged.

2.8-arcsec diameter aperture. However Filippenko's (1989) picture of NGC 4615 in Hα light and that of Della Valle et al. (1988) in the continuum show that SN 1987F lies to the north-west of a strong H II region in the same spiral arm. Therefore it is possible that some contamination in the sharp narrow lines occurs in our spectra from that source.

All wavelengths given below are heliocentric as measured from the spectra, unless otherwise stated. Some spurious telluric features can sometimes appear, notably the effects of subtracting the strong 5577-Å night-sky line and the strong atmospheric absorption band near 6900 Å.

3 DESCRIPTION OF THE SPECTRUM OF SN 1987F

3.1 The light curve and continuum

As relatively little photometry of SN 1987F is available, we estimated $(B-V)$ from our spectra. The 1.3-m instrumental setup provided good photometry generally and, although the nights were non-photometric so that we were unable to derive magnitudes reliably, the colours could be measured and thus the colour evolution of SN 1987F could be studied in

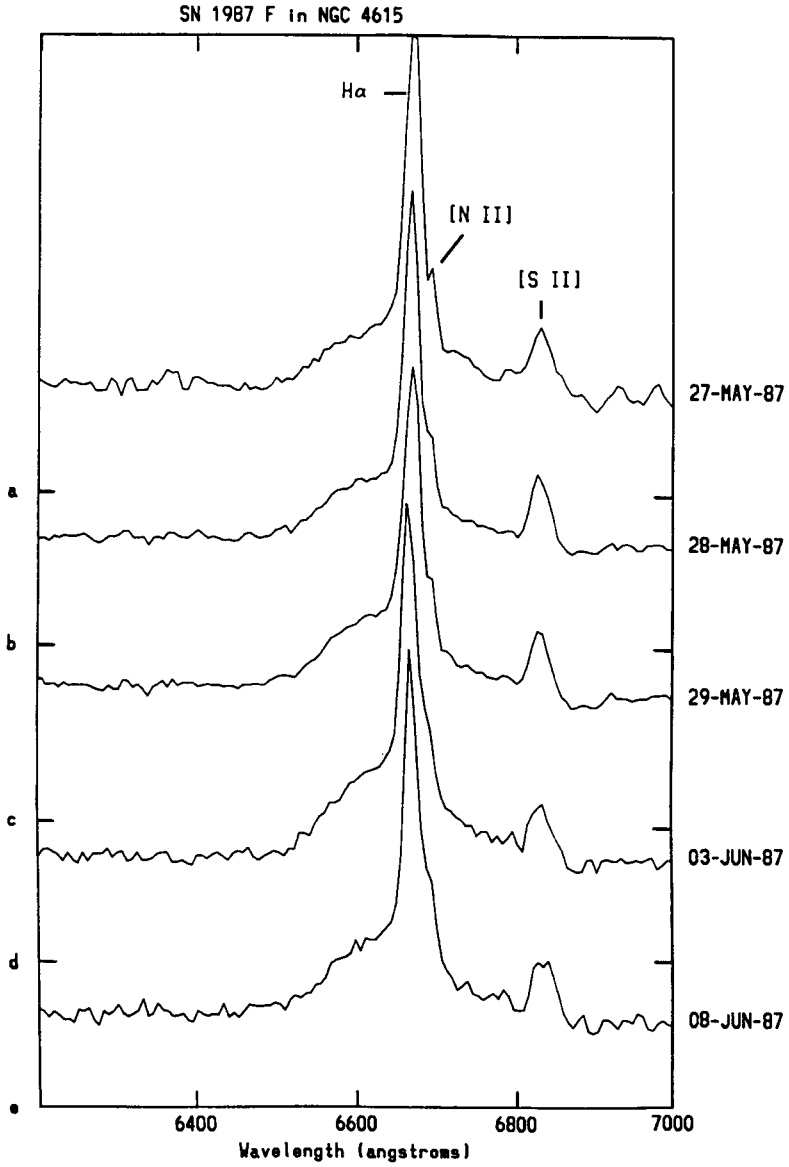

Figure 8. Enlargements of the Hα profiles from the same spectra as in Fig. 6. The positions of the narrow line components discussed in the text are marked. Zero intensity is denoted by the ticks marked a–e corresponding to each spectral registration running from the top to the bottom.

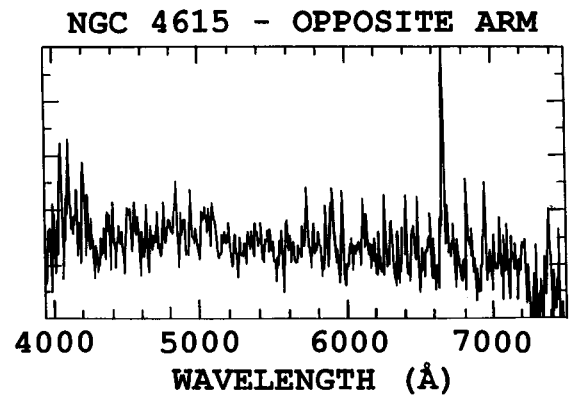

Figure 9. The spectrum of NGC 4615 obtained with the 1.3-m telescope on 1987 April 2. The entrance hole of the spectrograph was placed at the same distance from the nucleus as the supernova, but on the opposite spiral arm.

the earlier phases. The $(B-V)$ colours estimated from the monochromatic magnitudes at $B(\lambda 4300)$ and $V(\lambda 5500)$ were transformed using zero-points derived from standard stars observed nightly. For the 2.4-m 300 line mm^{-1} spectra, this could also be done, but less reliably, for B lies near the blue ends of the spectra. As the spectrum of the supernova was nearly continuous during these observations in the B and V bands, this method should be internally consistent. Seeing and refraction combined with the small apertures may also introduce additional error. Nevertheless, we estimate that the 1.3-m and 2.4-m $(B-V)$ colours given in Table 2 have internal accuracies of about ± 0.05 and ± 0.08 mag respectively.

The photographic light curves from published data described and referenced in the caption to Fig. 10 give $(B-V)$ bluer than those in Table 2 at the earliest phases. The broad B and V passbands can, however, be affected by

Table 2. $(B-V)$ colours for SN 1987F measured from the spectra.

H.J.D. -2440000	(B-V)
6887.79	+0.45
6888.80	+0.39
6890.74	+0.43
6892.70	+0.50
6893.69	+0.49
6895.66	+0.51
6896.66	+0.61
6899.68	+0.53
6900.67	+0.53
6901.67	+0.65
6902.66	+0.61
6903.66	+0.60
6905.70	+0.62
6942.63	+0.72
6943.63	+0.65
6944.63	+0.69
6949.63	+0.59

emission lines, background subtraction, and transformation errors, so for the present study we prefer to use the spectroscopic values of $(B-V)$; the results derived in Section 4.2 are not greatly affected by this choice.

Fig. 10 shows the V and B light curves of SN 1987F. Values are taken from the sources given in the figure caption and compared to the mean curves for SN 1988Z as discussed in Section 4.2.3. Fig. 11 shows the spectroscopic $(B-V)$ curve. There is no evidence for a plateau part of the V light curve. As Cappellaro et al. (1990) and Patat et al. (1993) have shown, neither standard SNe II-P nor SNe II-L light curves fit these data, even though there are no measures between JD 244 6975 and 244 7156. Furthermore, there are no pre-maximum observations, so the date and extent of the maximum light are poorly defined. Nevertheless, in V, SN 1987F appears to have been characterized by a linear light curve, while B shows some evidence for a change of slope after about 50 d which is consistent with the change in $(B-V)$.

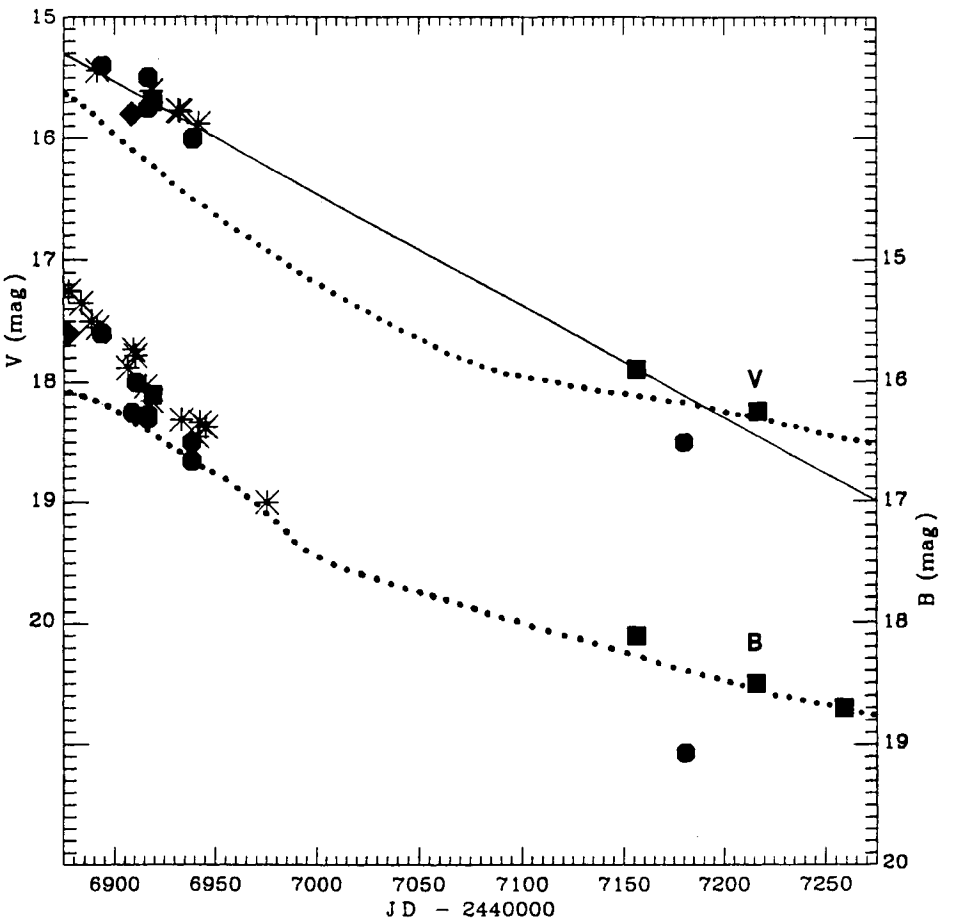

Figure 10. Photometry of SN 1987F. (Top) The V light curve. Symbols have the following meaning: (circle) Cappellero et al. (1990), (square) Filippenko (1989), (diamond) Wild & Schildknecht (1987), (asterisk) Tsvetkov (1989). (Bottom) The B light curve; symbols have the same meaning except diamond denotes an observation by Cherepaschuk et al. (1987). The solid line is the linear fit to the V data used in Section 4.2. The dotted curves give the corresponding mean light curves for SN 1988Z using Patat et al. (1993) adjusted for a difference of 0.74 mag in distance moduli.

3.2 The narrow emission lines

3.2.1 *Growth of the broad component*

Although the spectrum of SN 1987F as observed from 1987 April 2 to June 8 was not rich in strong features other than the H Balmer and [O III] lines in emission, changes occurred in their strengths and profiles as follows. (i) Starting with April 2, Figs 1 and 4 show that the emission lines were narrow, roughly the instrumental resolution in width, so probably unresolved. (ii) Beginning April 5, the 2.4-m spectra which have the higher signal-to-noise ratio, show an asymmetrical *red* wing developing in Hβ. At the same time, the narrow lines appeared to fade relative to the continuum and are hard to see in the 1.3-m spectra from April 10 and the Hα profiles remain sharp through April 20. (iii) With the second series of spectra obtained May 26 to June 8, in addition to the narrow emission lines, strong broad Balmer components have appeared. These are also seen in Filippenko's (1989) spectrum of May 5 bridging the two MDM series and persisted until at least 1988 April 7. The behaviour of broad [O III] λ5007 is difficult to judge owing to its possible blending with Fe II lines.

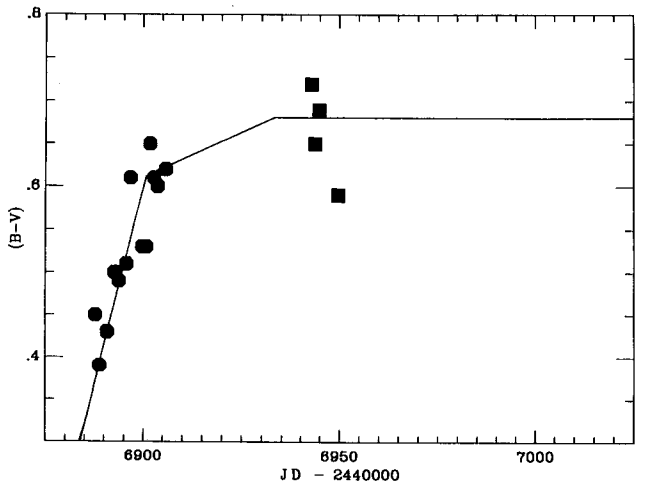

Figure 11. The $(B-V)$ curve with time determined from the MDM 1.3-m spectra, (circle) and 2.4-m spectra (square). The solid line segments indicate the fit to the data used in Section 4.2.

Measures of the wavelengths of the sharp components of Hα, Hβ and λ5007 in our series of observations indicate that they did not vary nightly by more than ± 92 km s^{-1} which is within the estimated error of the wavelength determinations for the measurement of a single line and yielded a mean redshift of 4861 ± 23 km s^{-1}. This is consistent with the value of 21 cm for NGC 4615 (de Vaucouleurs et al. 1991) if the difference of 147 km s^{-1} is primarily produced by the rotation of NGC 4615.

3.2.2 *Possible variations in the strength of [O III] relative to Hβ*

Several subtle changes also appear in the spectrum of SN 1987F. Before proceeding further we must emphasize the discussion in Section 2, which explains the difficulties in the interpretation of the narrow lines, owing to possible background contamination. One example is the behaviour of the narrow emission lines of Hβ and λ5007 of [O III]. Due to their proximity, the ratio of these lines should be relatively insensitive to changes in the slope of the continuum.

In Figs 1–3 and 4–5 the narrow lines fade relative to the continuum during 1987 April and indeed are hard to see in the 1.3-m spectra of April 14–16. This is accompanied by changes in the intensity ratio $R = I(\lambda 5007)/I(\mathrm{H}\beta)$ which are shown in Fig. 12. This shows nightly scatter but also an

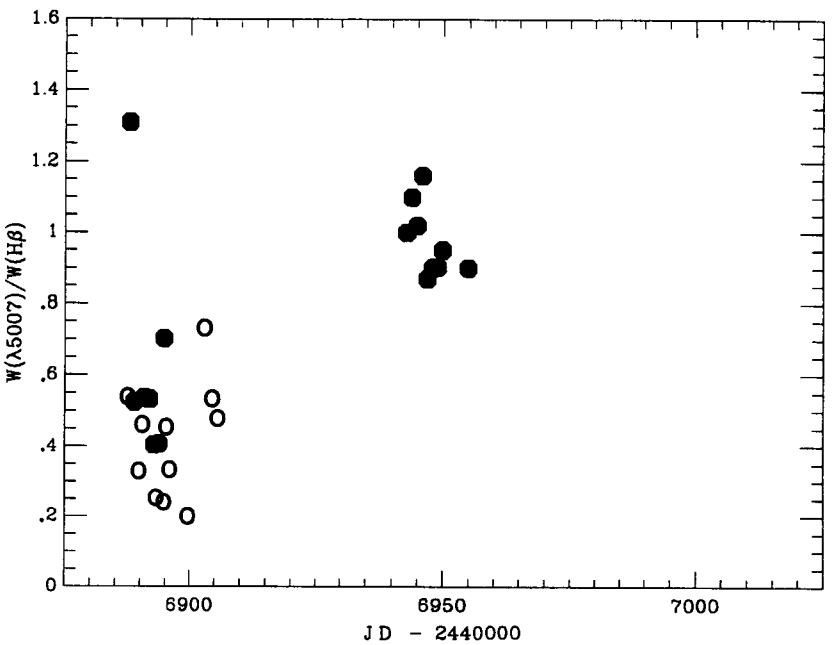

Figure 12. Changes in the ratios of the equivalent widths of the narrow line components of λ5007 and Hβ in the spectrum of SN 1987F. Open and filled circles denote data from the 1.3-m and 2.4-m telescopes, respectively.

increase in the mean R with time. The intensity of [O III] λ4959 also appears to track this behaviour.

Although random variations in the intensities of these narrow emission lines could be produced by placing the slit differently for each exposure, it is difficult to see how the lines would vary systematically in time, particularly when two different telescopes, one with a 1.9-arcsec slit and the other with a 2.8-arcsec diameter aperture, were employed, and saw the same effect. One 2.4-m spectrum obtained on April 2 is puzzling as it gives a very high value of R. As λ4959 also is higher in this spectrum, this does not appear to be instrumental, but suggests contamination by a background source. Furthermore the jump in R between 6900 and 6950 might signal changes in observing conditions between the two runs rather than real changes in the supernova, although none are apparent.

The increasing amount of [O III] indicated in Fig. 12 is consistent, however, with calculations made on a class of SN models where an expanding shock wave moves through the surrounding interstellar medium. Chevalier (1990), Lundqvist & Franson (1991) and Terlevich et al. (1992) have explored a range of models where the surrounding material was produced by mass-loss from a supergiant parent star or a dense homogeneous interstellar medium. Lundqvist & Franson (1991) obtain increasing [O III] for about the first 200 d in their models and all authors find evolution in the line strengths from their calculations.

Thus, although it is impossible to disentangle the contributions associated with the SN itself and the unresolved background, the changes in the intensities of the narrow components of Hβ and [O III] suggest that the narrow emission component of the spectrum of SN 1987F is not entirely produced by contamination from a nearby H II region. This question could perhaps be resolved by high-resolution imaging of the supernova environment in NGC 4615.

3.2.3 The forbidden N II and sulphur lines

The two blended [S II] lines, $\lambda\lambda$6716 and 6731, are present in many of the spectra at all epochs and give insight into the nature of the narrow line region. They appear in the 1.3-m observations of SN 1987F (Figs 1–3) where the signal-to-noise ratio is sufficiently high during 1987 April (e.g. April 2, 3, 5, 11 and 20), and in May–June they have a mean total equivalent width of 15 ± 2 Å. The [N II] λ6583 line shown in Fig. 8 during the latter period is clearly present on the red side of Hα but not well resolved. We estimate its equivalent width to be 9 ± 1 Å. At the same time, the narrow Hα equivalent width is 32 Å.

Using $\log([\mathrm{O\,III}]\,\lambda\,5007)/(\mathrm{H}\beta) \sim 0$ in Osterbrock's (1989) diagnostic diagrams, i.e. his figs 12.1 and 12.3, the relative line strength

$$\log([\mathrm{N\,II}]\,\lambda6583)/\mathrm{H}\alpha) \sim -0.8$$

places the narrow line component between the H II regions and emission line galaxies, while

$$\log([\mathrm{S\,II}]\,\lambda6716 + \lambda6731)/(\mathrm{H}\alpha) \sim -0.3$$

locates it similarly. Also, the absence of [O I] λ6300 in our spectra further suggests an H II region-like environment for the narrow lines. Although these [S II] lines are unresolved in our spectra (Fig 8), using Filippenko's (1989) spectra, $\lambda6716/\lambda6731 \sim 1.5$ indicates $N_e \sim 10^1$–10^2 cm^{-3}, using Osterbrock's (1989) fig. 5.3, which again suggests conditions more like those in an H II region rather than a hotter more exotic environment.

3.3 The broad Balmer line profiles and the reddening

The Hβ lines as observed with the 2.4-m telescope began to show a weak broad red wing after April 5 (Figs 4 and 7) which could not be seen in the noisier 1.3-m data. The blue wing of Hβ is definitely absent, but the presence of the extended red wing is consistent with a P Cygni profile for this feature at this early state. At the same time, this structure appears to be absent in the [O III] lines during April.

After 1987 May, the strengths of the broad Hα and Hβ lines in the spectrum of SN 1987F are striking. There is no evidence for a blue absorption component at later stages, although Filippenko's (1988) spectrum of May 5 shows weak blue absorption in the Hα profile.

Inspection of the profiles of the broad Hα and Hβ components in Figs 5 and 6 suggests different possible interpretations. For example, in Fig. 5, the profile of Hβ on the nights of May 30 and 31 and June 1 might be best fitted by a broad symmetrical profile blueshifted relative to the narrow lines, while on the nights of June 2 and 3, asymmetrical profiles stronger on the blue wing appear. For these lines in the spectrum of SN 1988Z Turatto et al. (1993) have fitted the sum of three Gaussian profiles of differing width, finding that the broadest component is blue shifted. The profiles of the Balmer lines are important for understanding the nature of the supernova and are discussed further in Section 4.1.

The reddening of SN 1987F is important in subsequent considerations on the nature of the supernova. This can be estimated to lie in the range of $A_B = 0.07$ and 1.7 mag. The mean equivalent widths of the broad components of Hα and Hβ in Fig. 6 were 129 Å and 30 Å respectively, or $I_{\mathrm{H}\alpha}/I_{\mathrm{H}\beta} \approx 4.3$ (for the narrow lines this is ~ 4.6). Using Osterbrock's (1989) 'c-method', if it is applicable, implies a colour-excess of $E(B-V) \sim 0.42$ or B-band absorption of $A_B \sim 1.7$ mag. This is larger than the total galactic and internal extinction given by de Vaucouleurs et al. (1991) which are $A_g = 0.07$ and $A_i = 0.49$ mag, respectively, and might imply some additional dust in the region of SN 1987F.

The Hγ line is relatively weak in our spectra of SN 1987F. It appears in the low-resolution 2.4-m spectra (Fig. 6) during May–June. The narrow component is present, but little can be said about the broad component in our data.

3.4 Other broad emission and absorption features

In addition to the emission lines above, a number of broad shallow emission and absorption bumps were seen in the spectra of SN 1987F.

3.4.1 Unidentified (5685 and 5178 Å)

In particular, an emission feature appears near λ5685 on April 11–20 (Figs 2 and 3). This has a rest wavelength near λ5594 and appears wider than the 8 Å resolution, suggesting a blend. A strong absorption near rest wavelength λ5093 appears in our later spectra. There are further hints of

transient features near the detection limit of the data. These include features near λ4700 on April 7 and 8 and λ6100 on several of the early nights (Fig. 1).

3.4.2 Fe II (4580 Å, 5250 Å)

Filippenko (1989) remarked on the presence of these broad features in the spectrum of SN 1987F during the later stages of its evolution and pointed out that these occur in QSO and AGN spectra (cf. Phillips 1977; Wills 1986). The development of these features is clearly visible in our MDM spectra after 1987 May 27. They are so broad that it is difficult to precisely judge their positions and the continuum level, but they extend roughly from $\lambda\lambda$5187–5653 and 4551–4755 with a mean equivalent width of 46 and 24 Å, respectively, during June 1–8.

The 4580 Å feature is a blend primarily due to multiplets 37, 38, and 43, while the 5250-Å region arises from multiplets 48 and 49. In addition, a peak near the rest wavelength of 5007 Å is produced by multiplet 42 (Phillips 1977). This also makes it difficult to decide about the origin of the broad feature near the [O III] λ5007 line. The equivalent width of this feature was 13 Å in early June. Further Fe II lines near $\lambda\lambda$6318 and 6384 owing to the $z^4D^0_{7/2} - c^4D_{7/2}$ and $z^4D^0_{5/2} - c^4D_{5/2}$ levels respectively can also be strong (Barrera, private communication) and may affect the region near the blue wing of Hα.

3.4.3 He I (5876 Å)

The earliest 2.4-m spectra probably show a weak narrow feature near λ5976 on most of the nights; the signal-to-noise ratios of the 1.3-m spectra are too low to show it. By May 27, a broad P Cygni profile appears to be present with a peak also near λ5976 and a trough near λ5886. The limit of the red wing is difficult to measure due to the line's weakness, but extends to about λ6150 corresponding to a velocity of $\sim$9000 km s^{-1} for some of the material, consistent with the value estimated from the Balmer lines. Equally difficult to estimate is the strength of the strong broad He I emission feature (cf. Fig. 7). For the May–June time interval, we find an equivalent width of $\sim$14 Å. Filippenko (1989) suggests that the absorption feature may arise from Na I λ5892 absorption in cool gas ejected before the explosion and for it we obtain an equivalent width of $\sim$4 Å.

4 ON THE NATURE OF SN 1987F

4.1 The Balmer line profiles

A notable aspect of the spectrum of SN 1987F is the strength of the broad Hα and Hβ lines and the absence of P Cygni absorption in the later times of its evolution. Filippenko (1989) and Chugai (1991) both remark on the asymmetry of these lines. There do not appear to be any realistic models of Type II supernovae published that can be directly applied to SN 1987F. Proper treatment of the problem requires solution of the non-local thermodynamic equilibrium (NLTE) radiative transfer with realistic geometry and density profiles (e.g. Höflich 1990). In a preliminary study, Chugai (1991) concluded that a broad asymmetrical Hα could be explained by a thin expanding shell with electron scattering. Such asymmetry is also a general feature of Type II supernovae as demonstrated by Best & Wehrse (1994) for artificial line models. Schlegel (1990) has considered the range of possibilities which include a dusty optically thin expanding spherical shell.

Inspection of the array of Hα and Hβ profiles and their time evolution suggests that both symmetric and asymmetric profiles can be fitted by such a simple mechanical model consisting of a radially expanding optically thin spherical shell with absorption. The line profiles produced by expanding rings, cones, and shells have been discussed extensively, e.g. by Schulz (1987) and Vrtilek (1983, 1985) and references therein. Since the profiles do not show strong double horns, it is concluded that a spherical shell geometry is a reasonable approximation, although not unique to such a shell. The absence of any P Cygni absorption in Hα after early May as discussed in Section 3.3 is consistent with the optically thin assumption. The expansion profile for an optically thick shell also gives a poorer fit (Unsöld 1968).

If we follow Vrtilek's (1983) model for a spherical shell of outer radius a, velocity law $v(r) \propto r^p$ and volume emissivity $\varepsilon \propto r^q$, and if there is absorption along the line of sight amounting to optical depth τ over a distance a, then the profile of an optically thin emission line will be

$$I(w) \propto \int_{\tilde{r}_{\rm in}(w)}^{\tilde{r}_{\rm out}(w)} \frac{\tilde{\varepsilon}(\tilde{r})\tilde{r}^2}{\tilde{v}(\tilde{r})} \times \exp\left\{-\tau\left[\sqrt{1-\tilde{r}^2\left(1-\frac{w^2}{\tilde{v}^2(\tilde{r})}\right)}+\frac{\tilde{r}w}{\tilde{v}(\tilde{r})}\right]\right\} \mathrm{d}\tilde{r} \qquad (1)$$

where the normalized radius is $\tilde{r} = r/a$ and $w = v/v(a)$. The limits $\tilde{r}_{\rm in}(w)$ and $\tilde{r}_{\rm out}(w)$ are set by the inner radius of the shell, δ, relative to a where the line of sight cuts through it. For a supernova outburst with homologous expansion, $v \sim r$ which fixes $p = 1$ and leaves δ, τ, and q to be determined.

As this simple model is only an approximation and since the individual profiles are both noisy and show variations, we decided to construct the mean profiles of Hα and Hβ for the May–June data, shown in Fig. 13, which could be used to make a rough estimate of these parameters. For both Hα and Hβ, the position of the narrow component was used to set the $w = 0$ or rest wavelength location. The profiles of May and June in Figs 5 and 8 were averaged, normalizing them to 1.0 at their peaks using the following continuum points: Hα ($\lambda\lambda$6450 and 6940), Hβ ($\lambda\lambda$4840 and 5025). The superimposed narrow lines had to be subtracted and this was done assuming that they have Gaussian shapes. The nightly variations may reflect deviations from a perfectly spherical expansion and contribute to the error bars in Fig. 13. Nevertheless, the resulting mean profiles both show asymmetry with stronger blue wings and agree reasonably in shape.

Examples of fits to the mean profiles of Hα and Hβ using equation (1) are also given in Fig. 13 for the MDM May–June data where the average phase is $t = 82$ d, the time for which subsequent estimates will be made. The horizontal bars in Fig. 13 show regions where, owing to the subtraction of the narrow lines, the data are unreliable. The Hα line is blended with the narrow components of [N II] and [S II] and is less reliable. Although weaker, the Hβ line was observed at higher resolution and the narrow component should affect the derived line profile and its asymmetry little (8000 km s^{-1} for the broad line versus less than 150 km s^{-1} for the

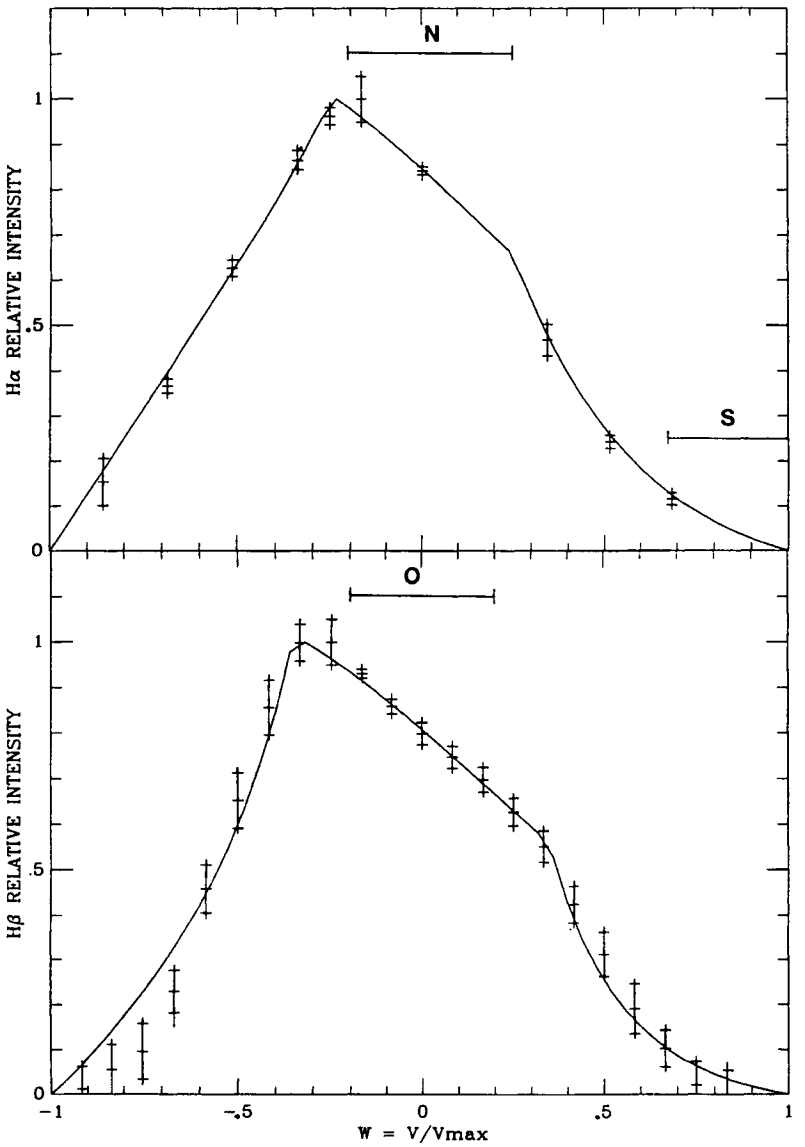

Figure 13. Fits to the mean observed Hα and Hβ profiles using equation (1), solid curves. The error bars show mean profiles derived from the data in Figs 5 and 8. The horizontal bars labelled 'N' give the approximate positions of the narrow H I + [N II] components, 'O' λ4959, and 'S' that of [S II] where the data were interpolated.

narrow). In addition, these line profiles can be compared with that of Hα derived by Chugai (1991) from Filippenko's (1989) data for $t = 150$ d.

The fit to the observed Hα and Hβ profiles in Fig. 13 shows reasonable agreements and the limitations of this simple model which can explain the asymmetries of the profiles. The turnover near $w = -0.3$ and 'knee' near $w = +0.3$ yield the value of $\delta = 0.35 \pm 0.1$. The red asymmetry of the profile sets $\tau = 0.85 \pm 0.1$, and the shape of the blue wings confines $q = -3.2 \pm 0.5$, where all fits and their errors are eye estimates. For Hα, $\delta = 0.25 \pm 0.1$, $\tau = 0.85 \pm 0.1$, and $q = -1.9 \pm 0.5$. The corresponding expansion velocities are $v(a) = 7400$ km s^{-1} and 8200 km s^{-1} for Hα and Hβ respectively.

The $v(a)$ should be relatively insensitive to the adopted line shape as it depends on the full width of the profile. Reduction of the asymmetry would lower the derived τ. The shell width parameter δ depends on the flatness of the top of the line profile, while q depends on the slope of the wings and both should not change much.

Similar fits can be made to the Hα profiles in fig. 3 of Filippenko (1989). The general shape and asymmetry of the profile appears to persist even though the line fades considerably after one year. For example, in the last two observations of Filippenko's (1989) series, the blue wing of Hα still appears higher than its weaker red counterpart.

The broad line profiles could be fitted differently in a more complicated manner, particularly for individual nights. One possible example is using the summation of wavelength-shifted symmetrical profiles as used by Turatto et al. (1993) for SN 1988Z. This would, however, probably require a more complex geometry than the one employed here and

defeat the purpose of trying to make rough estimates of the properties of the ejected shell from the mean profile and a simple model.

4.2 The physical parameters of SN 1987F

For subsequent calculations, we adopt a Hubble constant $H_0 = 75$ km s^{-1} and assume a solar composition in order to make some estimates of the physical properties of the supernova.

4.2.1 Spectroscopic shell mass

If the expansion rate is $v(a) \sim 8000$ km s^{-1}, then the mass and density of the expanding shell can be computed assuming homologous expansion and knowing its density in one layer. Filippenko's (1989) estimates of the logarithm of the mean electron density, $\log N_e \geq 9.0$, in early 1988 from the calcium and oxygen line ratios, constitute one such possibility, but may be insecure. According to his own rediscussion, Filippenko (1991) derives the mass of the emitting hydrogen to be $M \leq 0.1\ M_\odot$.

A second way to estimate the supernova's photospheric density is outlined by Hanuschik (1990). Assume that electron scattering dominates the continuum opacity. Then, the photospheric optical depth is

$$\tau_e \approx 1 = \int_{R_{ph}(t)}^{\infty} \sigma_e N_e(r, t)\, dr \qquad (2)$$

where $\sigma_e = 6.6 \times 10^{-25}$ cm^2. Assuming constant ionization in this region yields a density

$$\rho_1[R_{ph}(t)] \approx \mu m_p (\sigma_e \Delta v_n t_1)^{-1} (\tau_n^2 - \tau_{n-1}^2) \qquad (3)$$

where $\Delta v_n = v_{n-1} - v_n$, $v_n = R_{ph}(t_n)/t_n$, $t_1 = 1$ d, $\tau_n = t_n/t_1$, $\mu = 1.2$, and m_p is the mass of the proton, yielding $\rho_1 \approx 1.1 \times 10^{-9} \tau_n^{-3}$ g cm^{-3}, or $N_e \approx 1 \times 10^9$ cm^{-3} for SN 1987F at phase 82 d.

A third estimate of the density of the broad line region is Osterbrock's (1989) 'method B' for the recombination of hydrogen to the strength of the Hα line, $L_{H\alpha}$:

$$L_{H\alpha} \approx \left(\frac{4\pi j_{H\alpha}}{N_e^2}\right) N_e^2 V. \qquad (4)$$

Using $L_{H\alpha} = 1.4 \times 10^{40}$ erg s^{-1} and $v(a) \sim 8000$ km s^{-1} at $t = 82$ d, the volume is $V \sim 7 \times 10^{47}$ cm^3, and taking the term in brackets from Osterbrock's (1989) table 4.2, yields $N_e \approx 0.3 \times 10^9$ cm^{-3}, in reasonable agreement with the other two methods.

If the photosphere lies at the base of the broad-line-forming region, then since $v(r) \sim r$ and density $\rho \sim r^{-3}$, the mass of this outer shell is $M_{shell} \sim 0.2\ M_\odot$ and the kinetic energy is KE $\sim 1 \times 10^{49}$ erg. This holds for the broad-line-forming region above the photosphere and is a lower limit to these quantities for the entire supernova event. This may seem a surprisingly low mass for the shell, but could be consistent with SN 1987F having originated from a star whittled down by mass-loss which also produced the cloud of material giving rise to the narrow line region in the spectrum.

The radii determined from the bolometric luminosity and the above expansion velocity provide a useful check. For example, at a phase of 82 d and using $A_v = 1.3$ mag, the photometric radius calculated from $L_{bol} = 4\pi R_{ph}^2 \sigma T_e^4$ where $L_{bol} = 1.6 \times 10^{43}$ erg s^{-1} and $T_e = 8510$ K is $R_{ph} = 2.2 \times 10^{15}$ cm, while the expansion velocity at the *inner* edge of the shell, which we expect to more closely match the continuum, yields $R = v(t) \times \delta \times t = 1.7 \times 10^{15}$ cm. These radii could be brought into better agreement by small adjustments to the adopted H_0, the age since outburst, the reddening, the expansion rate, or all four so both methods give consistent values.

An additional complication is the question of the composition of the broad-line-region shell in SN 1987F. The equivalent width of He I λ5876 found in Section 3.4.3 relative to that of Hβ (30 and 14 Å respectively) indicates a higher than solar ratio of helium to hydrogen. Naively assuming that the regions of formation of the two lines are the same (Osterbrock 1989, p. 153) leads to the crude estimate that $N_{He^+}/N_p \sim 0.4$. Conversion of this to a He abundance requires choosing a temperature. If $T \sim 10\,000$ K, with $N_e = 10^9$ cm^{-3}, He would be 2.3 times more abundant than H. if $T \sim 20\,000$ K, the He is almost all He$^+$ and the lower limit of He:H ~ 0.4 is already approached. The absence of $\lambda\lambda$4686 and 5411 of He II in the spectrum of SN 1987F argue against He II being highly ionized, so we conclude that helium abundance could be enhanced in SN 1987F. Detailed models properly treating the radiative transfer and geometry are needed to check these estimates.

4.2.2 The bolometric light curve

The total luminous output of SN 1987F was very large because of its slow decay time and gives further information about the progenitor. Here we use the $(B-V)$ data in Table 2 and the V light curve to estimate the bolometric light curve on the assumption of the blackbody bolometric correction for the supernova.

From the V light curve in Fig. 10, we obtain

$$V = 15.24 \times 9.32 + 10^{-3}(t - 244\,6864.5) \qquad (5)$$

where the estimated time of outburst is 1987 March 10 (Filippenko 1989; Cappellaro et al. 1990) and the distance is $D = 63$ Mpc. Correction for reddening and using blackbody effective temperatures and bolometric corrections (Lamla 1965) as a function of the $(B-V)$ curve given in Fig. 11, gives a bolometric light curve and a total luminous energy for SN 1987F. Unfortunately, these are uncertain, owing to the poorly determined details of the reddening and the shape of the light curve, particularly for $t \leq 20$ d where V and $(B-V)$ had to be extrapolated. The resulting luminous energy is then $E_{rad} \sim 7 \times 10^{49}$ erg for $A_V = 0$ and $E_{rad} \sim 1 \times 10^{51}$ for $A_V = 1.3$ mag, which, as discussed in Section 3.3, should bracket the reddening. Nevertheless this is at least an order of magnitude larger than that of the famous Type II, SN 1987A (Catchpole et al. 1988).

Fig. 14 shows the corresponding bolometric light curves calculated from the photometry and blackbody bolometric corrections as described above. This is done for three values of A_V discussed in Section 3.3 where $A_V = 0$ and 1.3 should be lower and upper limits. After about day 60 BC is small, as T_e has dropped from $\sim 10\,000$ K on day 26 to ~ 7000 K

after day 60, where it remains nearly constant thereafter with $BC \sim 0.1$ mag. Consequently the hatched region in Fig. 14 is considered to be an estimate of the range permitted for the bolometric light curves.

Chugai (1991, 1992) has fitted the bolometric light curve of SN 1987F under the assumption that the main energy source is a result of the interaction of the expanding shock of the supernova and the circumstellar material lost from the precursor. Using older data to construct $L_{\rm bol}$, Chugai (1992) estimates that a shock model with an extremely dense superwind having wind density parameter $w = 2 \times 10^{17}$ g cm^{-1}, velocity 6000 km s^{-1} at 150 d, $E = 10^{51}$ erg, and shell mass, $M = 4\,M_\odot$ can fit the observations. The shape of $L_{\rm bol}$ is insensitive and as it is found to depend only weakly on shell mass M and energy E, and scales with w as $L_{\rm bol} \propto w^{1.5}$, it appears that a reasonable fit to $L_{\rm bol}$ can be achieved with this model as is shown in Fig. 14.

Chugai's (1991, 1992) estimate of $w = 2 \times 10^{17}$ g cm^{-1} is based on the radio properties of possibly similar SNe II and is higher than many of the actually observed objects. As indicated in Section 3.2, the [S II] optical line ratio indicates a lower density of material surrounding SN 1987F. Such material might also have further observational consequences which could be used to confirm its presence.

Terlevich et al. (1992) and Terlevich (1994) have derived analytical formulae for a somewhat similar simple model consisting of a peculiar Type II SN where the light curve is produced by the interaction of the shock wave from the SN ejecta with surrounding high-density homogeneous circumstellar material. This indicates that $L_{\rm shock} \sim t^{-11/7}$ and gives much the same slope as Chugai's (1992) result. According to Aretxaga & Terlevich (1994) the observed light curve of SN 1987F is not that of the supernova itself, but results from the luminous expanding shockwave which becomes visible about one year after the outburst.

The light curve of SN 1987F is, however, also fitted well with the $^{56}\mathrm{Ni} \rightarrow {}^{56}\mathrm{Co} \rightarrow {}^{56}\mathrm{Fe}$ decay chain for $t \geq 60$ d. Young & Branch (1989) have discussed the late tails of Type II supernovae being powered by ^{56}Co, where the energy deposition at time t is

$$L(t) = M_0(^{56}\mathrm{Ni})\{3.9 \times 10^{10} \exp(-t/T_{\rm Ni}) + 6.7 \times 10^{9}[\exp(-t/T_{\rm Co}) - \exp(-t/T_{\rm Ni})]\}\ \mathrm{erg\,s^{-1}}. \quad (6)$$

$M_0(^{56}\mathrm{Ni})$ is the ^{56}Ni mass, $T_{\rm Ni} = 8.8$ d and $T_{\rm Co} = 111.3$ d (Hanuschik 1990). Equation (6) assumes that all decay energy in the form of γ-rays is converted to optical radiation that immediately escapes. As Colgate, Petschek & Kiese (1980), Ensman & Woosley (1988), and Höflich, Müller & Khokhlov (1993) have shown, this depends in a complicated way on the expansion rate, distribution of the ^{56}Ni, and the γ-ray opacity in the supernova. If the ejecta are optically thin the γ-rays escape and equation (6) overestimates $L(t)$.

For large times, ^{56}Co decay drives $L(t)$ and this agrees well with the slope of the V light curve in Fig. 10 when converted to $L_{\rm bol}$ and shown in Fig. 14. $T_{\rm Co}$ implies a V decay of about 9.7×10^{-3}, close to the 9.3×10^{-3} mag day^{-1} slope of equation (5).

Naïve application of equation (6) indicates a large amount of ^{56}Ni. The upper curve shown in Fig. 14 is fitted by a mass of $M_0(^{56}\mathrm{Ni}) = 2.8\,M_\odot$, the middle yields $1.2\,M_\odot$, while no reddening gives $0.8\,M_\odot$. If we increase H_0 to 100 with $A_V = 0$ then this requires $0.4\,M_\odot$, while for $H_0 = 50$ and $A_V = 0$, $1.8\,M_\odot$ is needed. The total radioactive energy predicted from equation (6) and fits to the curves in Fig. 14 is $E_{\rm rad} = 0.1$–0.5×10^{51} erg. Summation of shock and decay curves

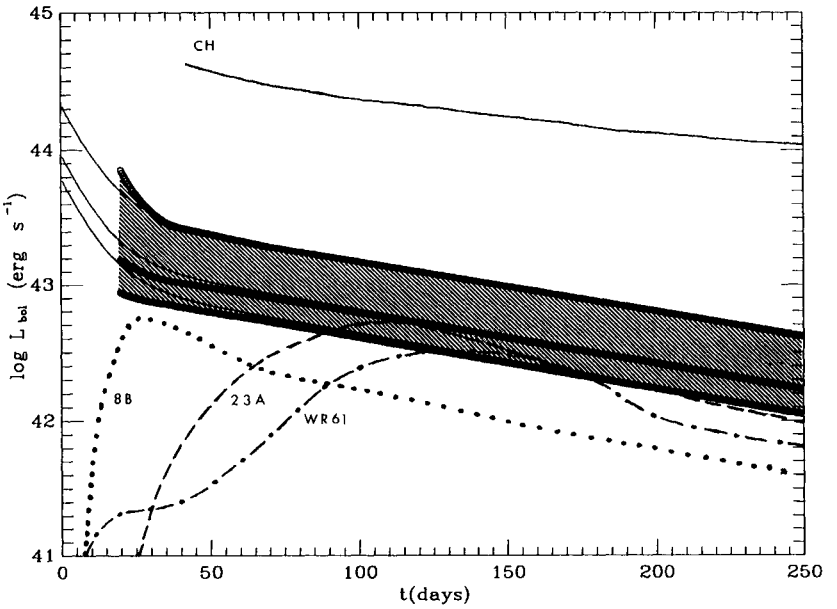

Figure 14. The bolometric light curves of SN 1987F constructed as described in Section 4.2.2 from V and $(B-V)$ photometry (thick solid curves) for different values of the reddening: $A_V = 1.3$, 0.5, and 0 mag (top to bottom). The thin solid curves are the luminosity predicted by equation (6) for the radioactive decay of ^{56}Ni and ^{56}Co for $M_0(^{56}\mathrm{Ni}) = 2.6\,M_\odot$ and the hatched area is what is considered permitted by observation. Some further model light curves are given for comparison: (8B) and (23A) 8 and 23 $M_\odot$ Wolf–Rayet models from Ensman & Woosley (1988); (WR61) 61 $M_\odot$ Wolf–Rayet model of Herzig et al. (1990); (CH) shock model of Chugai (1992) for $w = 2 \times 10^{17}$ g cm^{-1}, shifted vertically by 2.0.

lowers the required amount of $M_0(^{56}\mathrm{Ni})$, so this gives an upper limit to the radioactive contribution.

4.2.3 *Comparison with SN 1988Z*

SN 1988Z appears to be closely related to SN 1987F, but some differences are also seen. SN 1988Z has a better light curve and a longer time-base. Stathakis & Sadler (1991), Patat et al. (1993) and Turatto et al. (1993) have described the observations. Chugai & Danziger (1994) have interpreted SN 1988Z as being produced by the interaction of a strong shock with lumpy material surrounding the supernova from prior heavy mass-loss. With this model, they also get a low value for the expelled mass as was found in Section 4.2.1 for SN 1987F.

The light curves of SN 1987F and SN 1988Z are compared in Fig. 10. SN 1988Z may not have been quite as luminous as SN 1987F and its later decline is slower. Nevertheless for $t = 60$–215 d, it may fit with the decay of ^{56}Co, but would require a mass lowered by ~ 2 relative to SN 1987F. These earlier authors conclude a relatively low original mass of 8–$10\,M_\odot$ for SN 1988Z.

4.2.4 *Possible progenitors for SN 1987F*

Without more data and specific models, it is difficult to estimate the initial mass and the total energy for SN 1987F at present. Any model which explains this object must make use of a relatively low-mass, H-rich outer envelope expanding into a surrounding lower-density region. Also, it must produce the high luminosity and either the large amount of ^{56}Ni indicated from the light curve, or the slow decrease in light with this half-life by another process. Gaskell (1992) has discussed some of the possible mechanisms for Type II-L supernovae. Because of its peculiarities, SN 1987F is not fitted by any of the presently available models and thus the entire range of possibilities for supernovae should be considered. Light curves of some published models are plotted in Fig. 14 and are commented upon below.

(i) Although SN 1987F is classed as a Type II supernova, the models for Type Is would come closer to explaining a high mass of ^{56}Ni that may be required by the light curve. Most carbon detonation and deflagration models for Type I supernovae are capable of producing enough ^{56}Ni (e.g. Woosley 1990; Höflich et al. 1993; Khokhlov, Müller & Höflich 1993), but calculations with realistic radiative transfer do not produce high enough luminosities after about 60 days. Nomoto (1982) has, however, shown that 'double detonation' models produce sufficiently large amounts of ^{56}Ni (viz. 0.8–$1.4\,M_\odot$) and energy by incinerating a white dwarf and completely disrupting it. Iben & Renzini (1983) have proposed a 'Type $1\frac{1}{2}$', which, while much like the Type I models, also shares some of the properties of the Type II. The presence of ^{56}Co would help determine whether or not SN 1987F was produced by such a lower-mass progenitor.

(ii) A Type II-P supernova is characterized by a relatively massive H-rich outer envelope and as discussed, e.g. by Popov (1993) and references therein, the plateau stage is produced by hydrogen recombination, its duration and brightness depending on the mass and initial conditions of the explosion. The lack of a plateau in the light curve of SN 1987F suggests that the envelope did not provide a large amount of recombination energy and thus has a low hydrogen mass which is possibly also the case for the Type II-L supernovae.

(iii) The models for Type II-L supernovae by Swartz, Wheeler & Harkness (1991) also are generally not luminous enough. Of the three kinds of models that they consider, those utilizing carbon deflagration again come closest to producing the light curve of SN 1987F, while the massive-star core collapse and electron-capture-induced core collapse models, which they conclude as fitting Type II-L supernovae, produce too low luminosity. Blinnikov & Bartunov (1993) and Chugai (1990) have considered different models for the Type II-L's in which they employ non-equilibrium radiative transfer in a shock-heated extended circumstellar envelope from the pre-supernova wind to produce the luminosity. These models again fall well below SN 1987F in luminosity.

(iv) For massive stars and exotic scenarios, other problems in matching the light curve of SN 1987F exist. Wheeler (1990) has reviewed calculations of the evolution of massive supernovae. Ensman & Woosley (1988) have considered lower-mass Wolf–Rayet star progenitors. Herzig et al. (1990) have computed the light curve of an exploding $61\,M_\odot$ Wolf–Rayet star. The amount of ^{56}Ni produced depends critically on conditions in the supernova, but their light curve in Fig. 14 shows a rise time too slow and underluminous. Massive stars with Fe cores do not seem to produce enough ^{56}Ni in general. Woosley & Weaver's (1982) hypernova models would produce enough energy, but appear to have differently shaped light curves.

(v) It is unlikely that SN 1987F is a luminous blue variable undergoing mass-loss as an alternative explanation. Goodrich et al. (1989) have described the properties of Zwicky's (1965) Type V supernova, SN 1961V. This object was interpreted as an η Car type superoutburst of a massive evolved star near the end of H core burning. This explanation works for neither SN 1988Z nor SN 1987F. As Stathakis & Sadler (1991) point out, this predicts a constant bolometric luminosity, but as these two supernovae have nearly constant $(B-V)$ colours after $t \sim 60$ d and still fade, this requires a variable L_{bol}.

5 CONCLUSIONS

5.1 Conclusions from this investigation

Although at first sight the early spectrum of SN 1987F shown here appeared relatively simple, closer inspection reveals a complicated changing spectrum.

(i) The *narrow-line* component showed possible changes in the intensities of the sharp lines, notably as intensity variations of [O III] relative to Hβ, but interpretation is difficult owing to the possible contamination by the nearby H II region. The excitation of the narrow-line component resembles more an H II region.

(ii) The *broad-line* component is seen in the strong H I Balmer emission profiles and the wide blends attributed to Fe II. The development of the spectrum can be traced in Hβ where an extended red wing first appears, indicating a P Cygni profile which also is shown in an early published spectrum of Hα, but after May 27 this vanishes and is replaced by strong broad profiles in Hα and Hβ.

(iii) The simple mechanical model utilizing a thin expanding spherical shell with absorption can fit the broad parts of these profiles and indicates that the expansion speed of the shell's outer edge was ~ 8000 km s^{-1} from 1987 May 27 to June 8, about 82 d after the outburst.

(iv) This expansion velocity and three estimates of the mean density of the expanding shell yield a mass of $\sim 0.2\,M_\odot$ and kinetic energy of 1×10^{49} erg for the broad-line-region shell of the supernova, which appears to have an enriched abundance of helium. This is essentially independent of the shape of the profiles.

(v) The light curve, particularly *V*, appears nearly linear, shows no plateau phase, and indicates a total luminous output of $\sim 1 \times 10^{51}$ erg. This is consistent with a relatively low-mass hydrogen envelope.

(vi) The later phase of the light curve is fitted by the radioactive decay of ~ 0.8–$2.6\,M_\odot$ of ^{56}Ni, but it is also consistent with the shockwave model (Chugai 1992; Chugai & Danzier 1994; Terlevich 1994) if the circumstellar density is sufficiently high.

(vii) Even the spectral class of SN 1987F is open to question. Formally the star is SN Type II due to the Balmer lines in its spectrum. However, the He emission and other lines are unusual for this class of object (Branch 1990; Harkness & Wheeler 1990).

Taking the above into account, the following seems the best summary of the properties of the progenitor of SN 1987F. (1) Although not directly demonstrated by these observations, the data on the narrow line component do not contradict the assumption of earlier investigators who assumed considerable mass-loss before explosion producing the narrow-line region. The change in [O III] relative to Hβ may provide a clue to this. There is a suggestion of the physical conditions of an H II region from the other diagnostics, however. (2) A relatively low mass ($\sim 0.2\,M_\odot$) hydrogen envelope was ejected, which produced the broad Balmer lines and lack of a plateau stage in the light curve, also consistent with the mass loss. (3) Either carbon deflagration or detonation of the progenitor core producing enough ^{56}Ni, combined with interaction between the expanding shock front and the surrounding circumstellar material, are needed to explain the slow light curve. This and the lack of a broad slow maximum in the light curve may suggest a lower-mass progenitor ($M \leq 10\,M_\odot$) for SN 1987F.

Compared with other supernovae, according to Imshennik & Popov (1992), models for SN 1987A give $M \sim 15\,M_\odot$ and $E \sim 10^{51}$ erg, while a typical Type II-P supernova would have $M \sim 10\,M_\odot$ and $E_{\rm total} \sim 10^{51}$ erg (Litvinova & Nadëzhin 1985). For SN 1987A, the mass of the ^{56}Ni is estimated to be $\sim 0.07\,M_\odot$ (Arnett et al. 1989).

5.2 On the relationship of SN 1987F with AGNs

SN 1987F and others like it have been cited as a possible link and confirmation of the active galactic nucleus model of Terlevich et al. (1992 and references therein) which invokes supernova remnants expanding into a dense circumstellar environment during the later stages of a starburst process. This is a testable theory which Filippenko (1992) has reviewed giving its possible successes and problems, again pointing out the resemblance between the spectra of Type I Seyfert nuclei and SN 1987F.

Although the line strengths and continuum in SN 1987F resemble those observed in AGNs, in detail there are differences which may hint at difficulties in such an interpretation of this star. Furthermore, Wehrse & Shaviv (preprint) have shown that models of SN II and accretion discs around massive black holes can give comparable spectra at moderate resolutions due to the coincidence that pressure, temperature, and velocity can be similar in the line-forming regions of each.

There are at least three problems that arise from SN 1987F and its peculiar spectrum. The first is the shape of the line profiles, e.g. of Hα. For Type II supernovae, these must always be asymmetric to the red, while in many Seyfert Is they appear symmetrical. The second is concerned with the time-scale of the development of the strong broad emission lines. These were first seen roughly on 1987 May 3, ~ 50 d after the outburst. If the total lifetime of the broad-line era is ~ 400 d, then about 10 per cent of the lifetime of the event will be without strong lines. This means that at least for this type of supernova, a blue continuum phase without any strong broad emission lines will be present. It is also of interest to note that the large ^{56}Ni mass, if correct, would predict a high abundance of Fe in the AGNs. Finally, the third problem is that the narrow-line spectrum shows no evidence for an extensive high-density ($N_{\rm p} > 10^7$ cm^{-3}) environment around the supernova. If this were indeed the case, SN 1987F should have been an intrinsically strong radio source (Chugai 1991).

5.3 Possible further observations

Any additional photometric observations of SN 1987F would be extremely valuable. If the object came from a massive star, it may have been visible for many weeks or even months before 1987 March 22. Also if the shockwave theory developed by Aretxaga & Terlevich (1994) is responsible, an earlier outburst should have been visible about one year earlier. Archival optical and radio observations should be checked for at least upper limits. Further observations of the environment and remnant of SN 1987F would further help check its nature. If as much Fe as predicted from the light curve was produced, the remnant should have an interesting spectrum. Further atmospheric and explosion models that might help better understand SN 1987F would also be useful in order to better refine the crude estimates of composition and shell mass attempted here.

ACKNOWLEDGMENTS

GW acknowledges partial support by the National Science Foundation Grant AST93-47714, the SERC for a stay in Oxford at the Department of Astrophysics, and the Alexander von Humbolt-Stiftung for the opportunity to work at the Astronomisches Institut in Bochum. We are grateful to Dr Hartmut Schulz for patiently explaining line profiles and extensive advice and to Messrs E. Sutorius and M. Werger and Drs R. W. Hanuschik and R. A. Fesen for discussions. This work was based in part on research done at the MDM Observatory, operated by the University of Michigan, Dart-

mouth College, and the Massachusetts Institute of Technology.

REFERENCES

Aretxaga I., Terlevich R., 1994, MNRAS, 269, 462
Arnett W. D., Bahcall J. N., Kirshner R. P., Woosley S. E., 1989, ARA&A, 27, 629
Barbon R., Ciatti F., Rosino R., 1979, A&A, 72, 287
Best M., Wehrse R., 1994, A&A, 284, 507
Blinnikov S. I., Bartunov O. S., 1993, A&A, 273, 106
Branch D., 1990, in Petschek A. G., ed., Supernovae. Springer-Verlag, New York, p. 30
Cappellaro E., Della Valle M., Iijima T., Turatto M., 1990, A&A, 228, 61
Catchpole R. M., et al., 1988, MNRAS, 231, 75P
Cherepaschuk A. M., Metlova N., 1987, IAU Circ. 4370
Cherepaschuk A. M., Metlova N., Wheeler J. C., Kirshner R. P., Crotts A., McMahan R. K., Wegner G., Swanson S., 1987, IAU Circ. 4381
Chevalier R. A., 1990, in Petschek A. G., ed., Supernovae. Springer-Verlag, New York, p. 91
Chugai N. N., 1990, Sov. Astron. Lett., 16, 457
Chugai N. N., 1991, MNRAS, 250, 513
Chugai N. N., 1992, SvA, 36, 63
Chugai N. N., Danziger I. J., 1994, MNRAS, 268, 173
Colgate S. A., Petschek A. G., Kiese J. T., 1980, ApJ, 237, L81
Della Valle M., Cappellaro E., Ortolani S., Turatto M., 1988, ESO Messenger, 52, 16
de Vaucouleurs G., de Vaucouleurs A., Corwin H. G., Buta R. J., Paturel G., Foqué P., 1991, Third Reference Catalogue of Galaxies, Vol. III. Springer-Verlag, Berlin, p. 88
Doggett J. B., Branch D., 1985, AJ, 90, 2303
Ensman L. M., Woosley S. E., 1988, ApJ, 333, 754
Filippenko A. V., 1989, AJ, 97, 726
Filippenko A. V., 1991, in Woosley S. E., ed., Supernovae. Springer-Verlag, Berlin, p. 467
Filippenko A. V., 1992, in Duschl W. J., Wagner S. J., eds, Physics of Active Galactic Nuclei. Springer-Verlag, Berlin, p. 345
Filippenko A. V., Schachter J., 1988, IAU Circ. 4529
Gaskell C. M., 1992, ApJ, 389, L17
Goodrich R. W., Stringfellow G. S., Penrod G. D., Filippenko A. V., 1989, ApJ, 342, 908
Hanuschik R. W., 1990, Thesis Dr. rer. nat. habil., Ruhr-Universität Bochum
Harkness R. P., Wheeler J. C., 1990, in Petschek, A. G., ed., Supernovae. Springer-Verlag, New York, p. 1
Herzig K., El Cid M. F., Fricke . J., Langer N., 1990, A&A, 233, 462
Höflich P., 1990, Thesis Dr. rer. nat. habil., Ludwig-Maximilians-Universität, München
Höflich P., Müller E., Khokhlov A., 1993, A&A, 268, 570
Iben I., Jr., Renzini A., 1983, ARA&A, 21, 271
Imshennik V. S., Popov D. V., 1992, SvA, 36, 251
Khokhlov A., Müller E., Höflich P., 1993, A&A, 270, 223
Lamla E., 1965, in Voigt H. H., ed., Landolt-Börnstein Zahlenwerte und Funktionen aus Naturwissenshcaften und Technik. Neue Serie, Vol. 1, Springer-Verlag, Berlin, p. 369 (in German)
Litvinova I. Yu., Nadëzhin D. K., 1985, Sov. Astron. Lett., 11, 145
Lundqvist P., Franson C., 1991, ApJ, 380, 575
Maker S., Kurtz M. J., LaSala J., 1982, The REDUCE/INTERACT Package. Dartmouth College Dept. Physics & Astronomy, Hanover, NH
Nomoto K., 1982, ApJ, 257, 780
Osterbrock D. E., 1989, Astrophysics of Gaseous Nebulae and Active Galactic Nuclei. University Science Books, Mill Valley, p. 209
Patat F., Barbon R., Capellaro E., Turatto M., 1993, A&AS, 98, 443
Phillips M. M., 1977, ApJ, 215, 746
Popov D. V., 1993, ApJ, 414, 712
Schechtman S. A., Hiltner W. A., 1976, PASP, 88, 960
Schlegel E. M., 1990, MNRAS, 244, 269
Schulz H., 1987, A&A, 178, 7
Stathakis R. A., Sadler E. M., 1991, MNRAS, 250, 786
Swartz D. O., Wheeler J. C., Harkness R. P., 1991, ApJ, 374, 266
Terlevich R., 1994, Compact supernova remnants, RGO preprint No. 190
Terlevich R., Tenorio-Tagle G., Franco J., Melnick J., 1992, MNRAS, 255, 713
Tody D., 1986, Proc. SPIE, 627, 733
Tsvetkov D. Yu., 1989, Sov. Astron. Lett., 15, 129
Turatto M., Capellaro E., Danziger I. J., Benett S., Gouiffes C., Della Valle M., 1993, MNRAS, 262, 128
Unšold A., 1968, Physik der Sternatmosphären. Berlin, Springer-Verlag, p. 519 (in German)
Vrtilek J. M., 1983, PhD thesis, Harvard Univ.
Vrtilek J. M., 1985, ApJ, 294, 121
Wegner G., Swanson S. R., 1988, BAAS, 20, 962
Wegner G., Swanson S. R., 1990, AJ, 99, 330
Wehrse R., Shaviv G., 1994, preprint
Wheeler J. C., 1990, in Wheeler J. C., Pirani T., Weinberg S., eds, Supernovae. World Scientific, Singapore, p. 1
Wild P., Schildknecht T., 1987, IAU Circ. 4374
Wills B. J., 1986, in Viotti R., Vittone A., Friedjung M., eds, Physics of Formation of Fe II Lines Outside LTE. Reidel, Dordrecht, p. 161
Woosley S. E., 1990, in Petschek A. G., ed., Supernovae. Springer-Verlag, Berlin, p. 182
Woosley S. E., Weaver T. A., 1982, in Rees M. J., Stoneham R. J., eds, Supernovae: A Survey of Current Research. Reidel, Dordrecht, p. 79
Young T. R., Branch D., 1989, ApJ, 342, L79
Zwicky F., 1965, in Aller L. H., McLaughlin D. B., eds, Stellar Structure. Univ. Chicago Press, Chicago, p. 367